

Analysis of beryllium poisoning effect on liquid metal reactor with U–Be alloy fuel

Xiao-Liang Zou^{1,2} · Yun-Qing Bai¹ · Ming-Huang Wang¹ · Bing Hong^{1,2}

Received: 29 September 2017/Revised: 24 July 2018/Accepted: 16 August 2018/Published online: 29 January 2019
© China Science Publishing & Media Ltd. (Science Press), Shanghai Institute of Applied Physics, the Chinese Academy of Sciences, Chinese Nuclear Society and Springer Nature Singapore Pte Ltd. 2019

Abstract A liquid metal reactor (LMR) loaded with a fuel compound of uranium and beryllium (U–Be alloy fuel), which was cooled by a lead–bismuth eutectic alloy (PbBi), has been applied in Russian Alfa-class nuclear submarines. Because of the large amount of beryllium in the core, the reaction between the beryllium atoms and neutrons could result in the accumulation of ^3He and ^6Li , which are called the “poisoned elements” owing to their large thermal neutron capture cross section. The accumulation of neutron absorber can affect the performance of a reactor. In this study, the Super Multi-functional Calculation Program (SuperMC) code, which was developed by Institute of Nuclear Energy Safety Technology of the Chinese Academy of Sciences (INEST, CAS), was adopted to illustrate the influence of beryllium on an LMR.

Keywords LMR · U–Be alloy fuel · Beryllium poisoning · Super Multi-functional Calculation Program

1 Introduction

Lead-based reactors have attracted much attention because they are intrinsically safe and have high generating efficiency, mainly because of the inherent properties of lead coolant [1–5]. The first application of lead-based reactors in the world was Russian Alfa-class nuclear submarines in the 1960s, and the reactor, cooled by PbBi, was loaded with U–Be alloy fuel, in which the content of beryllium was as much as 90% [6]. With large amount of beryllium in the reactor, it was easier to achieve a reactor core with a smaller size and lower ^{235}U loading [7, 8]. In addition, beryllium had another type of reaction with gamma rays as a (γ, n) reaction to produce photoneutrons with the advantage of overcoming the instrumentation difficulty of the “blind zone” during reactor startup after any shutdown [9].

However, because of the large amount of beryllium in liquid metal reactor (LMR) core, except for the (n, n') reaction of beryllium atoms with neutrons as reflector and moderator, the reaction (n, α) was also significant with a cross section threshold energy only above 0.74 MeV. The nuclides ^3He and ^6Li , which were called “poisoned elements” because their large thermal neutrons capture a cross section of $5327 \times 10^{-24} \text{ cm}^2$ and $940 \times 10^{-24} \text{ cm}^2$, were generated by the interaction between the beryllium and neutron. The reactivity of the reactor continues to decrease with the increased neutron poisoning of poisoned element (^3He and ^6Li) accumulation. Many studies have been carried out on the beryllium poisoning effect. Omar et al. studied the effect of beryllium reflector poisoning on the Syrian MNSR [10]. Kalcheva et al. [11] illustrated the impact of the poisoning of the beryllium reflector on reactivity variations of the Belgian MTR BR2 in

This work was supported by the Natural Science Foundation of Anhui Province of China (No. 1608085ME107).

✉ Yun-Qing Bai
yunqing.bai@fds.org.cn

¹ Key Laboratory of Neutronics and Radiation Safety, Institute of Nuclear Energy Safety Technology, Chinese Academy of Sciences, Hefei 230031, Anhui, China

² University of Science and Technology of China, Hefei 230026, Anhui, China

SCK-CEN. Andrzejewski et al. [12] discussed beryllium poisoning in the MARIA reactor. However, all the research focused on the beryllium reflector, and no research was carried out on U–Be alloy fuel.

In this study, the analysis of the beryllium poisoning effect on an LMR with U–Be alloy fuel was investigated using the Super Multi-functional Calculation Program (SuperMC) code and MATLAB program. The LMR is introduced in Sect. 2. The computational tools and calculations are presented in Sect. 3. The results and discussion are given in Sect. 4. The conclusions are given in Sect. 5.

2 LMR description

The LMR was a prototype for the Alfa-class submarine, which had held the world record of nuclear submarine speed of 42 knots. The operation of the LMR started in September 1967 at 10% full power and lasted about 250 days [13]. The overall structural diagram of the LMR is shown in Fig. 1. The height and diameter of the LMR core were approximately 800 and 780 mm, respectively. A radial reflector was used, and it was composed of two layers of SS and a layer of BeO. Radial thermal shields of nine concentric cylinders were positioned around each reactor core between the outer surface of the reflector region and the inner surface of the reactor pressure vessel (RPV) wall. The nine concentric cylinders and the inner surface of the RPV wall were separated by, from the reflector region surface outward, nine annular PbBi coolant channels of 3-mm thickness each. Above the core was a special shield plug through which the 3 emergency protection rods, 10 control or compensation rods, and 24 emergency cooling tubes passed. There was approximately 300 mm of PbBi coolant between the top of the reactor

core and the reactor shield plug. Below the reactor were two cylindrical plates of the bottom thermal shield made of stainless steel (SS), from the lower core surface downward, with a 200 and 100 mm thickness, respectively. The lower cylindrical plate was adjacent to the inner surface of the RPV bottom and was separated from the upper cylindrical plate by a 100-mm-thick zone of the PbBi coolant.

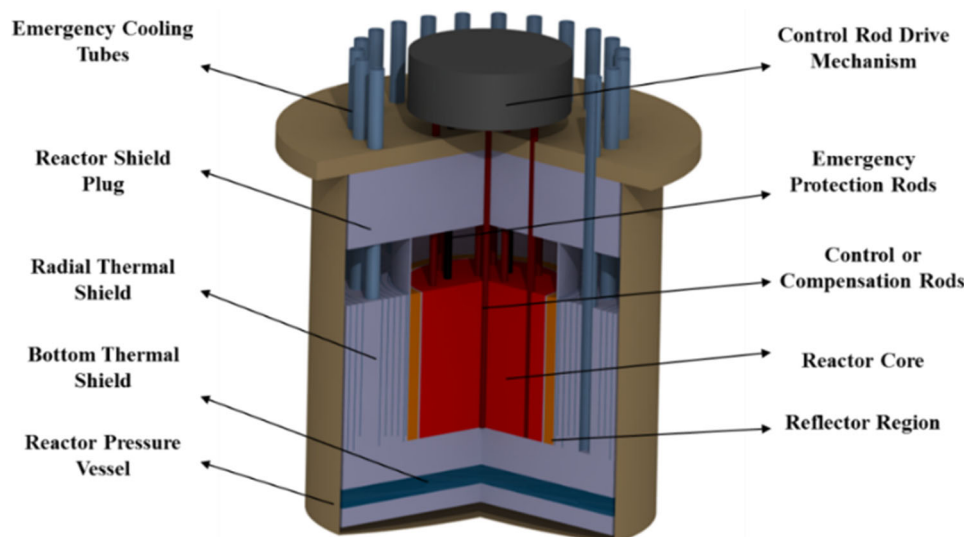
The LMR with a thermal power of 70 MW was loaded with 90 kg of ^{235}U . The fuel rod pellets, which were constructed of U–Be alloy in a BeO ceramic matrix, were approximately 10 mm in diameter. Therefore, this results in as much as 90% beryllium in the fuel. Lead–bismuth eutectic alloy, in which the content of lead was 44.5 wt% and of bismuth was 55.5 wt%, was used as the coolant in the LMR. The LMR had several advantages with a lead–bismuth eutectic alloy with a low melting point (approximately 125 °C) and high boiling point (approximately 1670 °C). It was safer and more compact than pressurized water reactors, because it operated at a low pressure with a less heavy pressure vessel. In addition, it could achieve a higher thermoelectric efficiency at a higher operational temperature. Typically, the distribution of LMR core materials was approximately 54% fuel, 36% PbBi, and 10% SS.

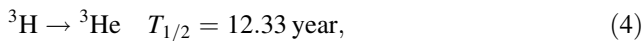
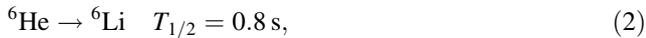
3 Computational tools and calculations

3.1 Basic equations

For the operation of the LMR, the neutron absorbers ^6Li and ^3He were accumulated in the reactor and had negative effects on reactivity [14]. The (n, α) reaction is described by the following equations:

Fig. 1 (Color online) LMR isometric view





The (n, α) reaction in Eq. (1) was a fast neutron reaction, and its threshold energy was approximately 0.74 MeV. The (n, α) reaction in Eq. (3) and the (n, p) reaction in Eq. (5) were thermal neutron reactions with cross sections of 945 barn and 5400 barn, respectively. In Eq. (2), the half time of ${}^6\text{He}$ was so short that ${}^6\text{Li}$ could be considered produced immediately in Eq. (1). Therefore, the number densities for each element could be obtained by solving the following equations:

$$\frac{dN_{\text{Be}}}{dt} = -N_{\text{Be}}R_{\text{Be}}, \quad (6)$$

$$\frac{dN_{\text{Li}}}{dt} = N_{\text{Be}}R_{\text{Be}} - N_{\text{Li}}R_{\text{Li}}, \quad (7)$$

$$\frac{dN_{\text{T}}}{dt} = N_{\text{Li}}R_{\text{Li}} - \lambda_{\text{T}}N_{\text{T}} + N_{\text{He}}R_{\text{He}}, \quad (8)$$

$$\frac{dN_{\text{He}}}{dt} = \lambda_{\text{T}}N_{\text{T}} - N_{\text{He}}R_{\text{He}}. \quad (9)$$

The notation N in above equations was used to simplify to represent the number densities. The subscripts Be, Li, T, and He stand for, respectively, ${}^9\text{Be}$, ${}^6\text{Li}$, ${}^3\text{H}$, and ${}^3\text{He}$. The constant λ_{T} was the tritium decay constant equal to $1.78 \times 10^{-9} \text{ s}^{-1}$. R stood for different reaction rates of the isotopes: (n, T) for ${}^6\text{Li}$, (n, p) for ${}^3\text{He}$, and (n, α) reaction for beryllium:

$$R_i = \int_0^{20} \varphi(E)\sigma_i(E)dE. \quad (10)$$

The energy of the neutrons in the reactor was in the range of 0–20 MeV, and $\sigma_i(E)$ was the relevant neutron-induced cross section for isotope i . Moreover, a MATLAB program [15] was used to solve the system of Eqs. (6)–(9) to get the number densities for lithium, tritium, and helium.

3.2 SuperMC calculation

In this research, the core analysis was performed by SuperMC with the Hybrid Evaluated Nuclear Data Library (HENDL). SuperMC, a general, intelligent, accurate, and precise simulation tool for the nuclear design and safety evaluation of nuclear systems, was designed by the FDS team in China [16, 17] to perform comprehensive neutronics calculation, taking the radiation transport as the core and including the depletion, radiation source

term/dose/biohazard, material activation and transmutation, etc., as shown in Fig. 2. SuperMC has been verified and validated by more than 2000 benchmark models and experiments, including ICSBEP and SINBAD [18, 19]. HENDL, a series of working nuclear data libraries developed by the FDS Team in China, has been applied in various applications pertaining to analysis of nuclear reactors. The accuracy of the library has been assessed and validated against various criticality safety and shielding benchmark experimental data [20].

The LMR core was modeled in three dimensions by the SuperMC code, and two different cross sections of the LMR are shown in Fig. 3. The SuperMC model was built according to the real dimensions of the LMR mentioned in the International Atomic Energy Agency (IAEA) report [18], and some simplifications were made. The SuperMC model consisted of four main parts: reactor core, radial reflector region, bottom thermal shield, and upper reflector region. The reactor core with an 800 mm height and 780 mm diameter was made of 54% U–Be, 36% PbBi, and 10% SS. The parameters used in the SuperMC simulation are listed in Table 1. The input file for SuperMC included 500 cycles made of 50 inactive and 450 active cycles with 20,000 histories per cycle. In this work, the flux, the reaction rate, and k_{eff} were calculated by the SuperMC calculation code. To normalize a criticality calculation by the steady-state power level of the reactor, the following conversion was used: $P(70 \times 10^6) \times 3.467 \times 10^{10} \times v(2.443) = 5.9 \times 10^{18}$.

4 Results and discussion

4.1 Time effects

Two calculation models were built for 250 days of full-power operation: (1) the one-step calculation model for one step of 250 days and (2) the five-step calculation model for five steps of 250 days and each step of 50 days. For the one-step calculation model, the initial reaction rate was obtained from the SuperMC calculation. Then, the reaction rates were assumed to be constant in the operation. For the five-step calculation model, first, the initial reaction rate was the same as for the one-step model. Then, the number density was calculated for 50 days (a step) by the MATLAB program. The number density in the SuperMC input file was updated in the next-step calculation.

The results of the calculations are presented in Fig. 4. For the one-step calculation model, constant reaction rates were used in the MATLAB program to make a relationship between the number density and the operation time, while reaction rates were changed for the next-step calculation in the five-step calculation model. As the figures show, for

Fig. 2 (Color online) Functional architecture of SuperMC

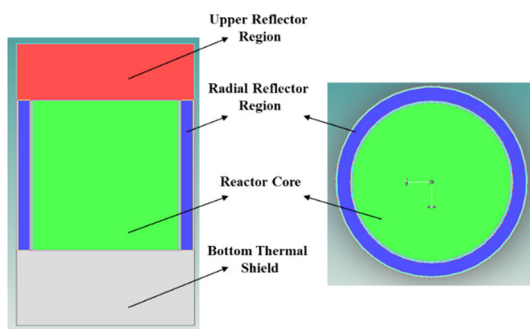
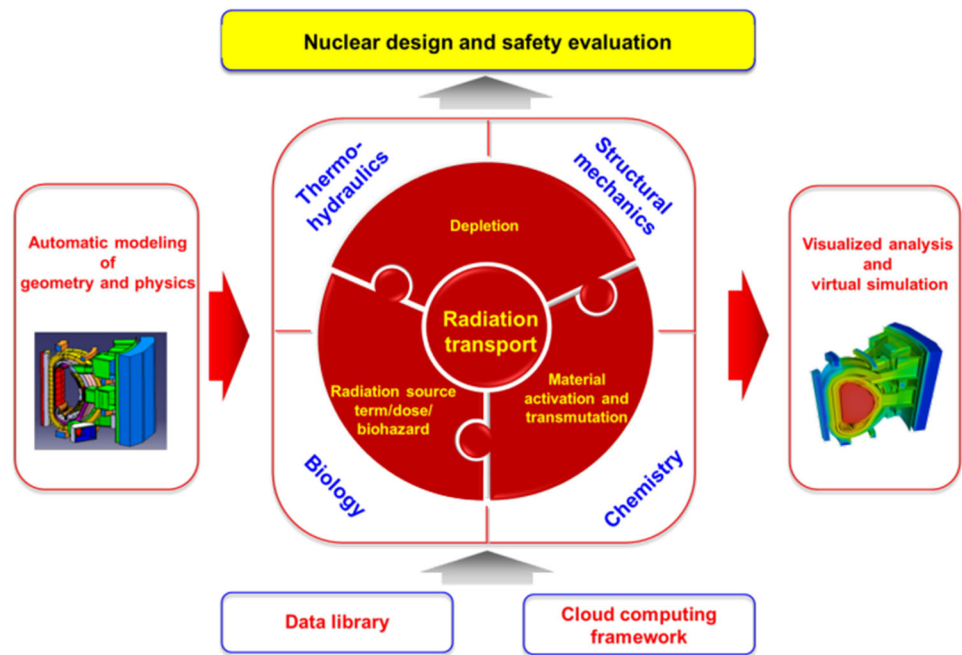


Fig. 3 (Color online) Vertical and horizontal cross sections of LMR using the SuperMC code

Table 1 Parameters of LMR SuperMC model

Items	Parameter (mm)	Materials
Reactor core		
Height	800	U–Be/PbBi/SS
Diameter	780	54%/36%/10%
Radial reflector region	10	SS
	65	BeO
	8	SS
Bottom thermal shield	200	SS
	100	PbBi
	100	SS
Upper reflector region	300	PbBi

both the one-step calculation model and the five-step calculation model, the number densities of the poisoned

elements, including ${}^6\text{Li}$, ${}^3\text{He}$, and ${}^3\text{H}$, continued increasing to the end of the period. For the one-step calculation model, the maximum values were 9.100×10^{18} , 1.575×10^{16} , and 1.913×10^{18} atoms/cm³, and they were 9.122×10^{18} , 1.564×10^{16} and 1.869×10^{18} atoms/cm³ for the five-step calculation model. Moreover, in the figures, the results of the one-step calculation model show good agreement with the five-step calculation model. This indicates that the poisoned elements accumulated in the LMR for 250 days of full-power operation showed almost no influence on the reaction rates. Figure 5 represents the fluxes for each step of the five-step calculation model, and they were almost the same for the poisoned element accumulation. The reaction rates were dependent on the flux in the reactor, which could explain why there was almost no difference among the results of the two calculation models. As a consequence, constant reaction rates were used for further study.

Figure 6 shows the poisoned element accumulation effect on k_{eff} for 250 days' operation of the LMR, in which clean for operation without the effect of the poisoned element accumulation, 10% power for actual operation, and full power for maximum-power operation. With the accumulation of the poisoned elements, k_{eff} continued to decrease for both 10% power and full-power operation except clean. It can be derived that the reactivity loss caused by the accumulation of the poisoned elements ${}^6\text{Li}$ and ${}^3\text{He}$ was approximately 98 pcm, which represented approximately 1.4% of the excess reactivity, while 1697 pcm represented 23.0% for full-power operation.

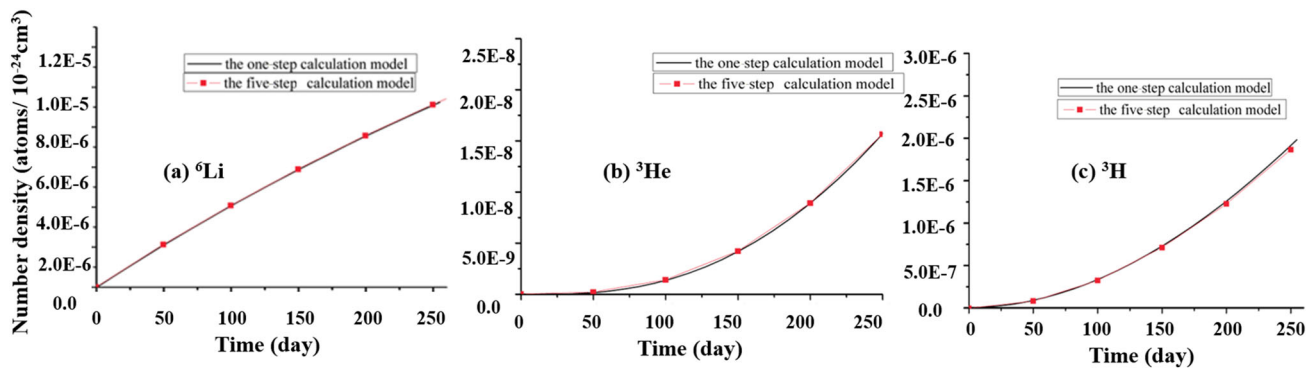


Fig. 4 Number density versus time: ⁶Li (a), ³He (b), and ³H (c)

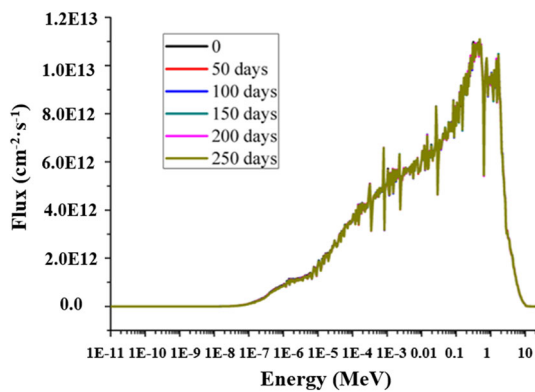


Fig. 5 Each step flux for the five steps calculation model

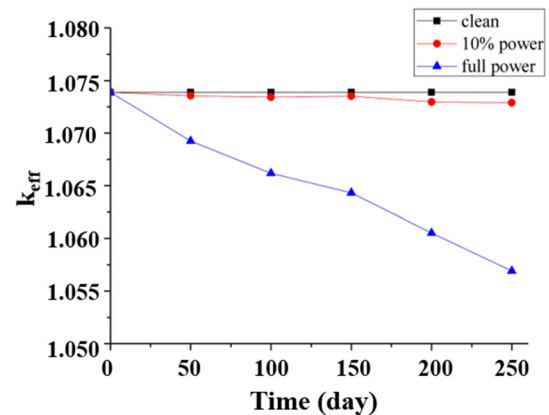


Fig. 6 Poisoned element accumulation effect on k_{eff}

4.2 Spatial effects

The magnitude and spectrum of the neutron flux have a direct influence on the poisoned element accumulation by the reaction rate. Therefore, the reaction rates depended on the position in the reactor. A detailed model was made to show the poisoned element accumulation for the different positions of the LMR core by dividing the LMR core from the radial direction into eight sections as follows:

- Section 1: radius from 0 to 5 cm
- Section 2: radius from 5 to 10 cm
- Section 3: radius from 10 to 15 cm
- Section 4: radius from 15 to 20 cm
- Section 5: radius from 20 to 25 cm
- Section 6: radius from 25 to 30 cm
- Section 7: radius from 30 to 35 cm
- Section 8: radius from 35 to 39 cm

The results of the calculations are presented in Fig. 7. The poisoned elements, including ⁶Li, ³He, and ³H, kept increasing in all sections, and the inside sections increased faster than the outside sections. Equation (10) indicates that the reaction rates that lead to the poisoned element accumulation depended on the flux distribution in the reactor. Figure 8 shows the flux distribution in the radial

direction. As can be seen, the flux of the inside sections was bigger than that of the outside sections, and this explains the result above.

In Fig. 7, one can also see that the difference between the inside sections was smaller than that of the outside sections. This was caused by the trend of flux variation with the radial direction, which decreased slowly first and then decreased sharply.

5 Conclusion

In this work, we focused on analysis of the beryllium poisoning effect on an LMR with U–Be alloy fuel. The beryllium poisoning effect was calculated by the SuperMC code and MATLAB program. The conclusions drawn from this study are as follows.

1. For actual operation for 250 days and 10% power, the reactivity loss caused by the accumulation of the poisoned elements ⁶Li and ³He was only 98 pcm, which represented approximately 1.4% of the excess reactivity, while 1697 pcm represented 23.0% for full-power operation.

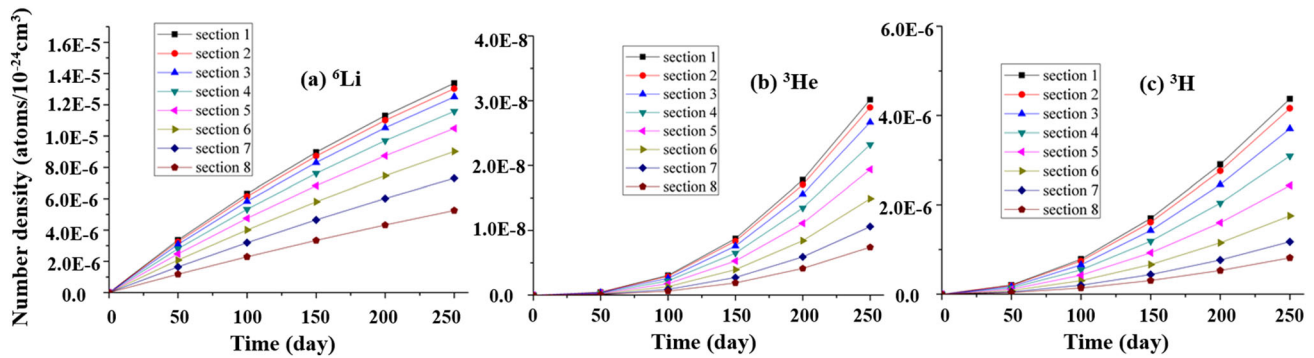


Fig. 7 (Color online) Number density versus time in different sections: ${}^6\text{Li}$ (a), ${}^3\text{He}$ (b), and ${}^3\text{H}$ (c)

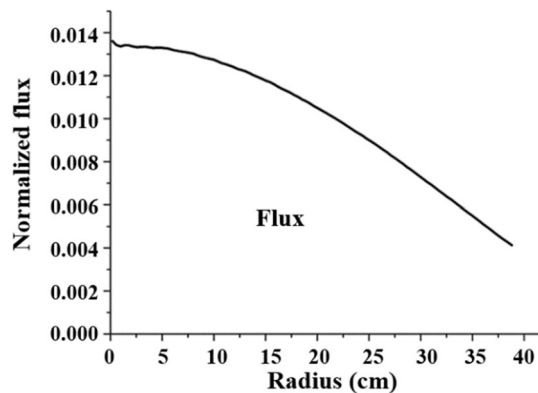


Fig. 8 Core radial distribution of flux

- In particular, the one-step calculation model and the five-step calculation model were used to perform the poisoned element accumulation effect on the generation of the poisoned elements later. The results showed that the effect of the accumulated poison elements could be neglected, because the flux and the power of the reactor were unchanging during 250 days of full-power operation.
- The spatial effects were researched by simulating with models dividing the reactor core into eight sections. The results showed that the poisoned elements accumulated in inside sections increased faster than those of outside sections, and the differences of inside sections were much smaller than those of outside sections because of the radial flux distribution.

The results show that the beryllium poisoning effect on an LMR with U–Be alloy fuel cannot be neglected. In the future, the effect should be taken into consideration when designing lead-based reactors with beryllium as a moderator or reflector.

Acknowledgements The authors would like to show their great appreciation to other members of the FDS Team in this research.

References

- Y.C. Wu, Y.Q. Bai, Y. Song et al., Conceptual design study on the China lead-based research reactor. *Chin. J. Nucl. Sci. Eng.* **2**, 201–208 (2014). <https://doi.org/10.3969/j.issn.0258-0918.2014.02.009> (in Chinese)
- Y.C. Wu, Y.Q. Bai, Y. Song et al., Development strategy and conceptual design of China lead-based research reactor. *Ann. Nucl. Energy* **87**, 511–516 (2016). <https://doi.org/10.1016/j.anucene.2015.08.015>
- Y.C. Wu, Design and R&D progress of China lead-based reactor for ADS research facility. *Engineering* **2**, 124–131 (2016). <https://doi.org/10.1016/J.ENG.2016.01.023>
- Y.C. Wu, J.Q. Jiang, M.H. Wang et al., A fusion-driven sub-critical system concept based on viable technologies. *Nucl. Fusion* **51**, 103036 (2011). <https://doi.org/10.1088/0029-5515/51/10/103036>
- Y.C. Wu, Z.P. Chen, L.Q. Hu et al., Identification of safety gaps for fusion demonstration reactors. *Nat. Energy* **1**, 16154 (2016). <https://doi.org/10.1038/nenergy.2016.154>
- O Reistad, P.L. Ølgaard, Russian nuclear power plants for marine applications (2006). <https://www.nks.org/scripts/getdocument.php?file=111010111120029>
- V.V. Kalygin, A.P. Malkov, V.V. Pimenov, Effect of ${}^3\text{He}$ and ${}^6\text{Li}$ accumulation in beryllium blocks on the neutron-physical characteristics of the MIR reactor. *Atom. Energy* **104**, 114–119 (2008). <https://doi.org/10.1007/s10512-008-9009-x>
- S. Glasstone, A. Sesonske, *Nuclear Reactor Engineering*, vol. 81 (Springer, Berlin, 1982), p. 3. <https://doi.org/10.1007/978-1-4615-2083-2>
- S.H. Sun, L. Zhu, H.T. Li, Research on nuclear properties of beryllium reflector in physical startup of reactor. *Nucl. Power Eng.* **36**, 14–17 (2015). <https://doi.org/10.13832/j.jnpe.2015.06.0014> (in Chinese)
- H. Omar, N. Ghazi, Kh Haddad et al., Study the effect of beryllium reflector poisoning on the Syrian MNSR. *Appl. Radiat. Isot.* **70**, 988–993 (2012). <https://doi.org/10.1016/j.apradiso.2012.02.118>
- S. Kalcheva, B. Ponsard, E. Koonen. Reactivity Effects due to Beryllium Poisoning of BR2 (PHYSOR 2004), Chicago, 25–29 April (2004)
- K. Andrzejewski, T. Kulikowska, M. Bretscher, et al., Beryllium poisoning in the MARIA reactor. *Beryllium* (2001). https://digital.library.unt.edu/ark:/67531/metadc720346/m2/1/high_res_d/789716.pdf
- N. Lynn, S. Timms, J. Warden, et al., Radionuclide release from submarine reactors dumped in the Kara Sea//Environmental impact of radioactive releases, in *Proceedings of An International*

- Symposium* (1995). https://www-pub.iaea.org/MTCD/Publications/PDF/te_0938_scr.pdf
14. K.J. Andrzejewski, T.A. Kulikowska, Z.E. Marcinkowska, Computations of fuel management in MARIA reactor with highly poisoned beryllium matrix. *Nukleonika* **53**, 173–179 (2008). https://www.nukleonika.pl/www/back/full/vol53_2008/v53n4p173f.pdf
 15. B.R. Hunt, J.M. Rosenberg, R.L. Lipsman, A guide to MATLAB: for beginners and experienced users. United Kingdom (2014). <https://doi.org/10.1017/cbo9780511791284>
 16. Y.C. Wu, F.D.S. Team, CAD-based interface programs for fusion neutron transport simulation. *Fusion Eng. Des.* **84**, 1987–1992 (2009). <https://doi.org/10.1016/j.fusengdes.2008.12.041>
 17. Y.C. Wu, J. Song, H. Zheng et al., CAD-based monte carlo program for integrated simulation of nuclear system SuperMC. *Ann. Nucl. Energy* **82**, 161–168 (2015). <https://doi.org/10.1016/j.anucene.2014.08.058>
 18. J. Song, G.Y. Sun, Z.P. Chen et al., Benchmarking of CAD-based SuperMC with ITER benchmark model. *Fusion Eng. Des.* **89**, 2499–2503 (2014). <https://doi.org/10.1016/j.fusengdes.2014.05.003>
 19. B. Zhang, J. Song, G.Y. Sun et al., Criticality validation of SuperMC with ICSBEP. *Ann. Nucl. Energy* **87**, 494–499 (2016). <https://doi.org/10.1016/j.anucene.2015.10.004>
 20. J. Zou, L.M. Shang, F. Wang et al., Development of a 1200 fine group nuclear data library for advanced nuclear systems. *Nucl. Sci. Tech.* **28**, 65 (2017). <https://doi.org/10.1007/s41365-017-0216-9>